Local kinetics of morphogen gradients

Peter V. Gordon[a], Christine Sample[b,c], Alexander M. Berezhkovskii[d], Cyrill B. Muratov[a,1], and Stanislav Y. Shvartsman[b,1]

[a]Department of Mathematical Sciences, New Jersey Institute of Technology, Newark, NJ 07102; [b]Department of Chemical Engineering and Lewis Sigler Institute for Integrative Genomics, Princeton University, Princeton, NJ 08544; [c]Emmanuel College, 400 The Fenway, Boston, MA 02115; [d]Mathematical and Statistical Computing Laboratory, Division of Computational Bioscience, Center for Information Technology, National Institutes of Health, Bethesda, MD 20892

Edited* by Iakov G. Sinai, Princeton University, Princeton, NJ, and approved February 18, 2011 (received for review December 22, 2010)

Some aspects of pattern formation in developing embryos can be described by nonlinear reaction–diffusion equations. An important class of these models accounts for diffusion and degradation of a locally produced single chemical species. At long times, solutions of such models approach a steady state in which the concentration decays with distance from the source of production. We present analytical results that characterize the dynamics of this process and are in quantitative agreement with numerical solutions of the underlying nonlinear equations. The derived results provide an explicit connection between the parameters of the problem and the time needed to reach a steady state value at a given position. Our approach can be used for the quantitative analysis of tissue patterning by morphogen gradients, a subject of active research in biophysics and developmental biology.

robustness | tissue regulation | concentration gradient

The formation of tissues and organs in a developing organism depends on spatiotemporal control of cell differentiation. This critical function can be provided by the concentration fields of molecules that act as dose-dependent regulators of gene expression, Fig. 1*A* (1). The idea that spatially distributed chemical signals can regulate developing tissues is more than 100 years old, but it was most clearly articulated in the 1969 paper by Wolpert (2, 3). Following his work, molecules acting as spatial regulators of development are referred to as *morphogens* and their distributions in tissues are called *morphogen gradients*. Morphogens remained a largely theoretical concept until the late 1980s, when morphogen gradients were visualized in the fruit fly embryo (4–7). At this point, morphogen gradients are recognized as essential regulators of embryonic development (8–11).

Morphogen gradients can form by reaction-diffusion mechanisms, the simplest of which is the so-called source–sink mechanism, whereby a locally produced molecule is degraded as it diffuses through the tissue (12–15). The source–sink model has been used to explain gradient formation in multiple developmental contexts, including the vertebrate neural tube, the embryonic precursor of the central nervous system. Neural tube is patterned by the gradient of locally produced extracellular protein Sonic hedgehog (Shh), which binds to cell surface receptors that both mediate cellular responses to Shh and regulate the range of its diffusion, Fig. 1*B* (16–18). Cells at different positions in the tube sense different levels of Shh, express different genes, and give rise to different neurons (19).

Although genetic and biochemical studies of morphogen gradients are very advanced, quantitative characteristics of morphogen gradients are relatively unexplored. In particular, the dynamics of morphogen gradients has been studied only in a handful of experimental systems and mathematical models (13, 20–31). This motivates our work, in which we present analytical results for the dynamics in reaction–diffusion equations based on the source–sink mechanism.

We consider a semiinfinite one-dimensional "tissue" ($x > 0$), in which a morphogen is produced at a constant rate Q at the boundary ($x = 0$), diffuses with diffusivity D, and is degraded according to some rate law. Production starts at time $t = 0$,

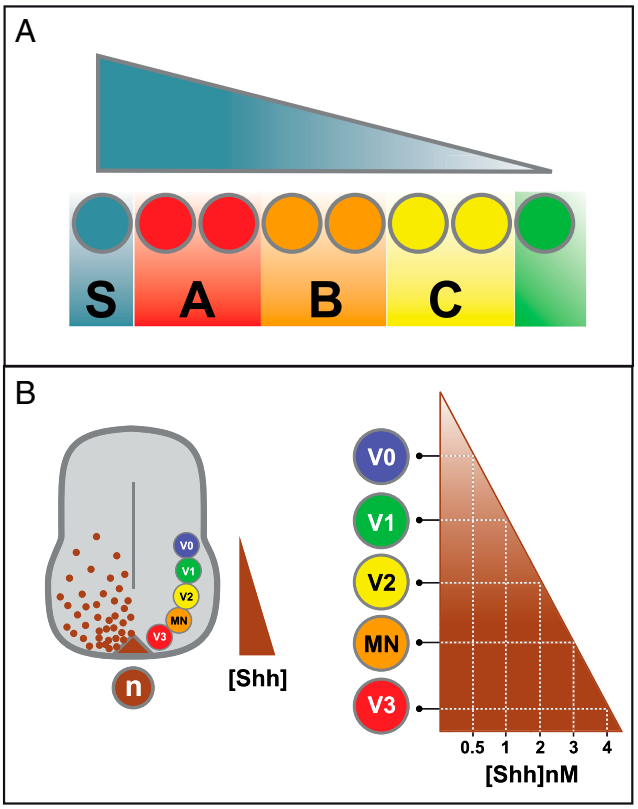

Fig. 1. A schematic picture of a one-dimensional morphogen gradient. (*A*) A secreted signal (blue) is produced from a localized source (S) and spreads through the tissue to establish a gradient. Cells respond to different concentrations of the signal by regulating different sets of genes (red, orange, and yellow). This induces distinct cell fates (*A*–*C*) at different distances from S. (*B*) Shh protein (brown) is produced from the notochord (n) and floor plate at the ventral midline of the neural tube. Shh spreads dorsally establishing a gradient that controls the generation of distinct neuronal subtypes [interneurons (V0–V3) and motor neurons (MN)]. In vitro, different concentrations of Shh are sufficient to induce the distinct neuronal subtypes. The concentration of Shh necessary to induce a specific subtype corresponds to its distance to the source in vivo. [Reproduced with permission from ref. 16 (Copyright 2009, Macmillan Publishers Ltd).]

when the morphogen concentration, denoted by $C(x,t)$, is zero throughout the system. The time evolution of $C(x,t)$ thus satisfies

Author contributions: P.V.G., C.S., A.M.B., C.B.M., and S.Y.S. designed research; P.V.G., C.S., A.M.B., C.B.M., and S.Y.S. performed research; P.V.G. and C.B.M. contributed new reagents/analytic tools; P.V.G., C.S., C.B.M., and S.Y.S. analyzed data; and P.V.G., C.S., C.B.M., and S.Y.S. wrote the paper.

The authors declare no conflict of interest.

*This Direct Submission article had a prearranged editor.

[1]To whom correspondence may be addressed. E-mail: muratov@njit.edu or stas@princeton.edu.

This article contains supporting information online at www.pnas.org/lookup/suppl/doi:10.1073/pnas.1019245108/-/DCSupplemental.

APPLIED MATHEMATICS

DEVELOPMENTAL BIOLOGY

$$\frac{\partial C}{\partial t} = D\frac{\partial^2 C}{\partial x^2} - k(C)C, \qquad C(x,t=0) = 0, \qquad [1]$$

$$-D\frac{\partial C}{\partial x}\bigg|_{x=0} = Q, \qquad C(x=\infty,t) = 0, \qquad [2]$$

where $k(C) > 0$ is the pseudo first-order rate constant of the degradation process.

The solution of the initial boundary value problem in Eqs. **1** and **2** approaches the steady state, denoted by $C_s(x)$, as $t \to \infty$, which commonly forms the basis for analyzing the experimentally observed morphogen gradients. At the same time, the extent to which experimentally observed gradients can be interpreted as the steady states of the underlying reaction–diffusion process is currently unclear (23, 32).

Following the classical paper by Crick (33), we address this question by estimating the time scale on which the concentration at a particular position x approaches its steady state value $C_s(x)$. If the cells at this position have to respond to the morphogen by some time that is considerably less than the time of local approach to the steady state, the tissue is patterned by a time-dependent gradient. In the opposite extreme, the tissue is patterned by the steady-state gradient.

The dynamics of local approach to the steady state can be characterized by the relaxation function, which is defined as the fractional deviation from the steady state at a given point (34); see Fig. 2:

$$R(x,t) = \frac{C(x,t) - C_s(x)}{C(x,0) - C_s(x)} = 1 - \frac{C(x,t)}{C_s(x)}. \qquad [3]$$

The fraction of the steady concentration that has been accumulated between times t and $t + dt$ is given by $-(\partial R(x,t)/\partial t)dt$, which can be interpreted as the probability density for the time of morphogen accumulation at a given location. Based on this, we have recently introduced the *local accumulation time* $\tau(x)$ that characterizes the time scale of approach to the steady state at given x:

$$\tau(x) = -\int_0^\infty t\left(\frac{\partial R(x,t)}{\partial t}\right)dt. \qquad [4]$$

We have demonstrated that accumulation time can be used to quantitatively interpret the dynamics of experimentally observed morphogen gradients (34). For linear reaction–diffusion models, i.e., when $k(C) = k_1$, an analytical expression for $\tau(x)$ can be derived from the analytical solution of the corresponding linear equation:

$$\tau_1(x) = \frac{1}{2k_1}\left(1 + \frac{x}{\sqrt{D/k_1}}\right). \qquad [5]$$

However, the approach used in ref. 34 no longer works for nonlinear models, which are frequently used in the current biophysical literature on morphogen gradients.

To deal with nonlinear problems, we developed a more general approach that leads to inequalities yielding universal upper and lower bounds for the local accumulation time. Importantly, these bounds explicitly depend on the parameters of the problem. For instance, as we show below, in the case of second-order degradation kinetics, i.e., when $k(C) = k_2C$:

$$\frac{1}{12}\left\{\left(\frac{12\sqrt{D}}{Qk_2}\right)^{1/3} + \frac{x}{\sqrt{D}}\right\}^2 \le \tau_2(x) \le \frac{1}{6}\left\{\left(\frac{12\sqrt{D}}{Qk_2}\right)^{1/3} + \frac{x}{\sqrt{D}}\right\}^2. \qquad [6]$$

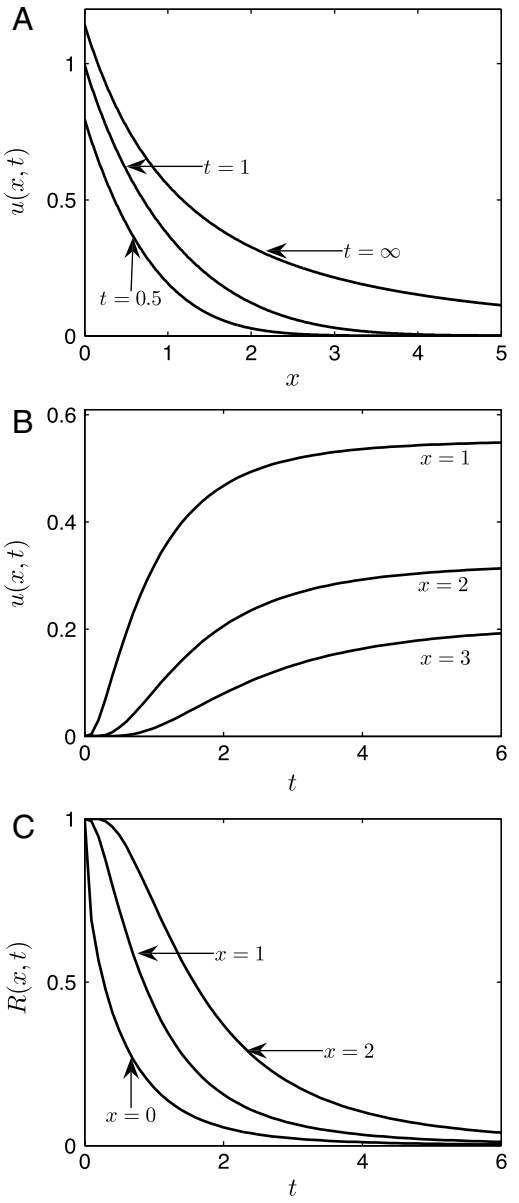

Fig. 2. Establishment of a one-dimensional morphogen gradient through production at the boundary, diffusion, and degradation. (*A–C*) Results from the numerical solution of Eq. **21**, the dimensionless problem with second-order degradation kinetics, where the dimensionless source strength is $\alpha = 1$. All numerical solution are obtained using the Crank–Nicolson method. (*A*) Concentration profiles for various times, where $t = \infty$ indicates the steady state $v(x)$ in Eq. **24**. (*B*) Concentration dynamics at three different values of x. The approach to steady state is faster for points closer to the source of production. (*C*) The relaxation function plotted for several values of x.

Below we demonstrate that such two-sided inequalities can be rigorously derived for several nonlinear reaction–diffusion problems. The derived results are in good quantitative agreement with the results obtained from numerical solution of the underlying nonlinear problems (Fig. 3).

Methods

Our main tool in the analysis of the initial boundary value problems in Eqs. **1** and **2** is the comparison principle for quasilinear parabolic equations, which is behind many intuitive insights for the considered class of problems (see, e.g., refs. 35–40). It gives rise to some strong monotonicity properties of solutions of these equations, which, in turn, can be used to analyze the solutions by explicitly constructing barrier functions that can lead to pointwise upper and lower bounds at all times.

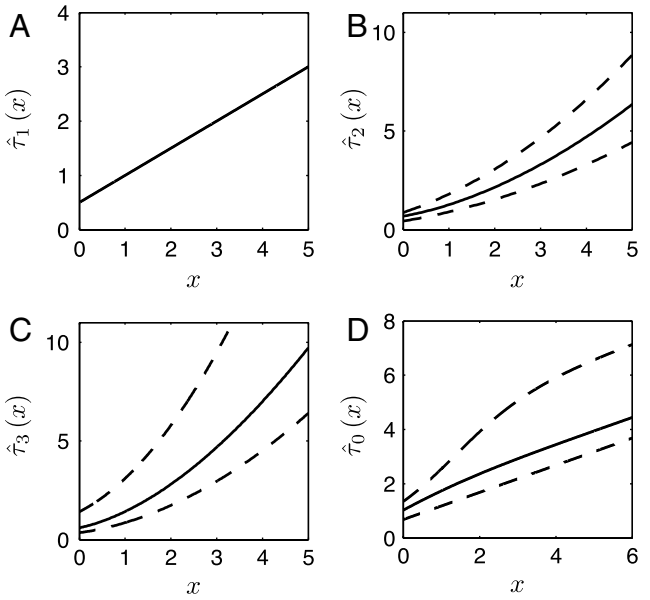

Fig. 3. Comparison of the analytical results of the dimensionless accumulation time $\hat{\tau}(x)$ defined through the right-hand side of Eq. **25** with those obtained from the numerical solution of the corresponding initial boundary value problems. In *A*–*C*, $u(x,t)$ solves Eq. **41**, with $n = 1,2,3$, respectively. In *D*, $u(x,t)$ solves Eq. **43**. In all cases, the dimensionless source strength $\alpha = 1$. In *A*, the accumulation time depends linearly on the distance from the source. In *B* and *C*, the accumulation time scales quadratically with distance. In *D*, the local accumulation time behaves linearly for large x.

Parabolic Comparison Principle. Consider the equation

$$u_t = u_{xx} + f(u,x,t), \qquad x > 0, \qquad [7]$$

where f is some sufficiently regular function of its arguments (see *SI Appendix* for precise assumptions and statements). We will denote by $\overline{u} = \overline{u}(x,t)$ a *supersolution* of Eq. **7**, i.e., a sufficiently regular function that satisfies the inequality

$$\overline{u}_t \geq \overline{u}_{xx} + f(\overline{u},x,t), \qquad x > 0. \qquad [8]$$

Similarly, we will denote by $\underline{u} = \underline{u}(x,t)$ a *subsolution* of Eq. **7**, i.e., a sufficiently regular function that satisfies the inequality

$$\underline{u}_t \leq \underline{u}_{xx} + f(\underline{u},x,t), \qquad x > 0. \qquad [9]$$

Now suppose that the following inequality for the super- and subsolution holds at the boundary

$$\underline{u}_x \geq \overline{u}_x, \qquad x = 0 \qquad [10]$$

and that $\overline{u}$ and $\underline{u}$ are ordered at the initial moment:

$$\underline{u} \leq \overline{u}, \qquad t = 0. \qquad [11]$$

Then we have the following basic result (see *SI Appendix* for the precise statement; see also refs. 37–40:

$$\underline{u} \leq \overline{u} \qquad \forall (x,t) \in [0,\infty) \times [0,\infty). \qquad [12]$$

Because the solution of Eq. **7** is both a super- and a subsolution, under the same type of assumptions on the initial and boundary conditions we obtain for all x and t:

$$\underline{u} \leq u \leq \overline{u}. \qquad [13]$$

Thus, $\overline{u}$,$\underline{u}$ serve as barriers for the solution $u(x,t)$. These functions can often be constructed explicitly, making the analysis of the considered nonlinear problems tractable.

As an illustration of the comparison principle, let us prove the intuitively obvious fact that the solutions of Eqs. **1** and **2** increase monotonically in time for every $x \geq 0$ and approach the steady state as $t \to \infty$. Indeed, for arbitrary $t_0 > 0$ we have $C(x,t_0) \geq 0 = C(x,0)$ for all $x \geq 0$. Therefore, applying the comparison principle with $\overline{C}(x,t) = C(x,t+t_0)$ and $\underline{C}(x,t) = C(x,t)$, we find that $C(x,t+t_0) \geq C(x,t)$, and in view of arbitrariness of t_0 the solution is a monotonically increasing function of t for each x (36). Similarly, the function $\overline{C}(x,t) = C_s(x)$ is a supersolution that remains above C for all x and t. So by uniqueness of the steady state C_s for a given Q and any $k(C) > 0$, we have $C(x,t) \to C_s(x)$ uniformly in x as $t \to \infty$ (see *SI Appendix* for details). This justifies the definition of the accumulation time $\tau(x)$ introduced in Eq. **4**.

Inequalities for the Local Accumulation Time. Together with the comparison principle, super- and subsolutions for Eq. **1** can be used to estimate the local accumulation time from above and below. Upon integration by parts Eq. **4** becomes

$$\tau(x) = \int_0^\infty R(x,t)dt = \frac{1}{C_s(x)} \int_0^\infty (C_s(x) - C(x,t))dt, \qquad [14]$$

which is justified as long as the right-hand side of Eq. **14** is bounded (see *SI Appendix* for more detail; this condition is found to be true in all the cases considered). As a consequence, given an ordered sequence $\underline{C}(x,t) \leq C(x,t) \leq \overline{C}(x,t)$, we have

$$\frac{1}{C_s(x)} \int_0^\infty (C_s(x) - \overline{C}(x,t))dt \leq \tau(x) \leq \frac{1}{C_s(x)} \int_0^\infty (C_s(x) - \underline{C}(x,t))dt. \qquad [15]$$

Now, let $C(x,t)$ be the solution of Eqs. **1** and **2**, and let $\underline{C}(x,t)$ and $\overline{C}(x,t)$ be the respective sub- and supersolutions, i.e., functions satisfying

$$\frac{\partial \underline{C}}{\partial t} \leq D\frac{\partial^2 \underline{C}}{\partial x^2} - k(\underline{C})\underline{C}, \qquad \underline{C}(x,t=0) = 0, \qquad [16]$$

$$\frac{\partial \overline{C}}{\partial t} \geq D\frac{\partial^2 \overline{C}}{\partial x^2} - k(\overline{C})\overline{C}, \qquad \overline{C}(x,t=0) = 0, \qquad [17]$$

and $-D\frac{\partial \underline{C}}{\partial x}|_{x=0} = -D\frac{\partial \overline{C}}{\partial x}|_{x=0} = Q$. Then the estimate in **15** follows immediately from the comparison principle. Below, we demonstrate the usefulness of the approach described above with explicit computations of the bounds in **15** for several well-established models of morphogen gradients.

Results

We now apply our approach to the case of the degradation rate obeying a superlinear power law:

$$k(C) = k_n C^{n-1}, \qquad n = 2,3,\ldots, \qquad k_n > 0. \qquad [18]$$

This model was proposed to describe the situation in which the morphogen increases the production of molecules which, in turn, increase the rate of morphogen degradation (41). For example, Shh induces the expression of its receptor patched, which both transduces the Shh signal and mediates Shh degradation by cells (17, 18).

We treat explicitly the case of the second-order degradation kinetics $n = 2$ below and then briefly discuss the analytical results for $n \geq 3$ (see *SI Appendix* for details). The obtained formulae are compared with the "exact" solutions obtained numerically.

Nondimensionalization and Steady State. For $n = 2$, the initial boundary value problem in Eqs. **1** and **2** is rendered dimensionless by the following transformation:

$$x' = \frac{x}{L}, \qquad t' = \frac{t}{T}, \qquad u = \frac{C}{C_0}, \qquad [19]$$

where

$$L = \left(\frac{D}{k_2 C_0}\right)^{1/2}, \qquad T = \frac{1}{k_2 C_0}, \tag{20}$$

and C_0 is a reference concentration that characterizes the threshold in the cellular response to the morphogenetic field and is introduced for convenience of the interpretation. Dropping the primes to simplify the notation, we arrive at the following dimensionless problem:

$$u_t = u_{xx} - u^2, \qquad u_x(0,t) = -\alpha, \qquad u(x,0) = 0, \tag{21}$$

where we introduced the dimensionless source strength

$$\alpha = \frac{Q}{\sqrt{D k_2 C_0^3}}. \tag{22}$$

The steady state $v(x)$ of this problem satisfies the equation

$$v_{xx} - v^2 = 0, \qquad v_x(0) = -\alpha, \tag{23}$$

whose explicit solution is

$$v(x) = \frac{6}{(a+x)^2}, \qquad a = \left(\frac{12}{\alpha}\right)^{1/3}. \tag{24}$$

We then define the dimensionless local accumulation time (cf. Eq. **14**)

$$\hat{\tau}_2(x) = \frac{1}{v(x)} \int_0^\infty [v(x) - u(x,t)]dt. \tag{25}$$

The corresponding dimensional local accumulation time is

$$\tau_2(x) = T\hat{\tau}_2(x/L). \tag{26}$$

Super- and Subsolutions. To proceed with our analysis, we slightly modify the steps leading to Eq. **15** and introduce the new variable $w = v - u$. It is easy to check that w satisfies the following problem:

$$\begin{cases} w_t = w_{xx} - (u+v)w & (x,t) \in (0,\infty) \times (0,\infty) \\ w_x(0,t) = 0 & t \in (0,\infty) \\ w(x,0) = v & x \in [0,\infty). \end{cases} \tag{27}$$

and decreases monotonically to zero for each x as $t \to 0$. We now explicitly construct super- and subsolutions for this problem. Consider uniformly bounded functions $\overline{w}$,$\underline{w}$ satisfying

$$\begin{cases} \overline{w}_t = \overline{w}_{xx} - v\overline{w}, & (x,t) \in (0,\infty) \times (0,\infty), \\ \overline{w}_x(0,t) = 0 & t \in (0,\infty), \\ \overline{w}(x,0) = v & x \in [0,\infty), \end{cases} \tag{28}$$

and

$$\begin{cases} \underline{w}_t = \underline{w}_{xx} - 2v\underline{w}, & (x,t) \in (0,\infty) \times (0,\infty), \\ \underline{w}_x(0,t) = 0 & t \in (0,\infty), \\ \underline{w}(x,0) = v & x \in [0,\infty). \end{cases} \tag{29}$$

Because $0 \le u \le v$, it is easy to see that $\overline{w}$,$\underline{w}$ satisfy the types of inequalities in **8** and **9**, respectively, and the same initial and boundary conditions as w. Therefore, by Parabolic Comparison Principle, we have

$$\underline{w} \le w \le \overline{w}, \tag{30}$$

for all $(x,t) \in [0,\infty) \times [0,\infty)$ and, hence,

$$\frac{1}{v(x)} \int_0^\infty \underline{w}(x,t)dt \le \hat{\tau}_2(x) \le \frac{1}{v(x)} \int_0^\infty \overline{w}(x,t)dt, \tag{31}$$

for all $x \ge 0$, which is analogous to **15**.

Upper and Lower Bounds for $\hat{\tau}_2(x)$. In contrast to the original equation, the equations for $\overline{w}$,$\underline{w}$ are *linear* and, therefore, are easier to study. In particular, we can apply the Laplace transform

$$\overline{W}(x,s) = \int_0^\infty e^{-st}\overline{w}(x,t)dt, \tag{32}$$

$$\underline{W}(x,s) = \int_0^\infty e^{-st}\underline{w}(x,t)dt, \tag{33}$$

to Eqs. **28** and **29** to obtain the following boundary value problems:

$$\overline{W}_{xx} - (v+s)\overline{W} = -v, \qquad \overline{W}_x(0,s) = 0, \tag{34}$$

$$\underline{W}_{xx} - (2v+s)\underline{W} = -v, \qquad \underline{W}_x(0,s) = 0. \tag{35}$$

This is justified for all $s > 0$ in view of the boundedness of $\overline{w}$,$\underline{w}$. Furthermore, in terms of the Laplace transform **31** takes an especially simple form:

$$\frac{\underline{W}(x,0^+)}{v(x)} \le \hat{\tau}_2(x) \le \frac{\overline{W}(x,0^+)}{v(x)}, \tag{36}$$

where in passing to the limit as $s \to 0^+$ we applied monotone convergence theorem (42) (note that a priori both bounds in **31** could also be infinite).

Both Eqs. **34** and **35** admit closed form analytical solutions. The formula for $\overline{W}(x,s)$ reads

$$\overline{W}(x,s) = \frac{6}{s(a+x)^2}\left(1 - \frac{2e^{-\sqrt{s}x}(s(a+x)^2 + 3\sqrt{s}(a+x) + 3)}{a\sqrt{s}(a^2 s + 3a\sqrt{s} + 6) + 6}\right), \tag{37}$$

where a is given in Eq. **24**. Note that this is a meromorphic function of $z = \sqrt{s}$ for each x and, therefore, admits a Laurent series expansion at $z = 0$. Performing the expansion, we find that this function is analytic in the neighborhood of zero, and

$$\overline{W}(x,0^+) = 1. \tag{38}$$

A similar computation can be performed in the case of $\underline{W}(x,s)$, yielding (the result can no longer be expressed in terms of elementary functions, but the same steps apply, see *SI Appendix*)

$$\underline{W}(x,0^+) = \frac{1}{2}. \tag{39}$$

Then, substituting Eqs. **38** and **39** into **36**, we obtain matching upper and lower bounds for the quantity $\hat{\tau}_2(x)$:

$$\frac{1}{12}(a+x)^2 \le \hat{\tau}_2(x) \le \frac{1}{6}(a+x)^2. \tag{40}$$

Because the obtained upper and lower bounds differ only by a factor of two, they should provide a good estimate of the

accumulation time computed on the basis of numerical solution of the original nonlinear problem. As shown in Fig. 3*B*, this is indeed the case.

Higher-Order Degradation Kinetics. We now briefly mention the results obtained for the dimensionless version of the problem in Eqs. **1**, **2**, and **18** with $n \geq 3$:

$$u_t = u_{xx} - u^n, \qquad u_x(0,t) = -\alpha, \qquad u(x,0) = 0. \qquad \textbf{[41]}$$

Defining $\hat{\tau}_n(x)$ to be the dimensionless accumulation time for a given value of n as in Eq. **25**, we performed a similar analysis for $n \geq 3$ (see *SI Appendix* for details). For example, we obtained that

$$\frac{a^3 + 2(x+a)^3}{12(x+a)} \leq \hat{\tau}_3(x) \leq \frac{a^2 + (x+a)^2}{2}, \qquad a = \left(\frac{2}{\alpha^2}\right)^{1/4}. \qquad \textbf{[42]}$$

A similar bound is found for $n = 4$ (see *SI Appendix*).

As can be seen from the obtained formulae, we have $\hat{\tau}_n(x) \sim x^2$ for $x \gg 1$ and $n = 2,3,4$. Let us point out that under this growth assumption the formulae for the bounds may be formally obtained by solving the analogs of Eqs. **34** and **35**, setting $s = 0$ and selecting the unique solution that yields the required growth. One needs to be careful, however, in applying this formal approach, because in the absence of a rigorous justification it can lead to incorrect results. For example, it can be shown that for $n \geq 5$ this approach produces negative upper bounds. This indicates that the solution of the analog of Eq. **34** diverges as $s \to 0^+$, and more sophisticated supersolutions need to be constructed to obtain meaningful bounds for $n \geq 5$.

Dependence on the Time Scales of Diffusion and Reaction. When morphogen degradation follows first-order kinetics [$k(C) = k_1$], the accumulation time $\tau_1(x)$ is given by Eq. **5**. From this expression it is clear that at distances exceeding the characteristic reaction–diffusion length scale $L = \sqrt{D/k_1}$, the accumulation time is given by the geometric mean of the times of reaction ($\tau_r \equiv 1/k_1$) and diffusion ($\tau_d \equiv x^2/D$): $\tau_1(x) \sim (\tau_r \tau_d)^{1/2}$. How is this scaling modified when the rate of morphogen degradation is a nonlinear function of concentration? Our results can be used to systematically address this question for problems with superlinear power-law degradation rates.

Back in the original scaling, the estimates derived for $\tau_2(x)$ take the form given by Eq. **6**. Based on this equation, for large x we have $\tau_2(x) \sim \tau_d \equiv x^2/D$; i.e., the local accumulation time is governed solely by the diffusion time scale. It is easy to see that this is also true in the cases $n = 3,4$, where the upper and lower bounds were derived analytically (see *SI Appendix*). The results for $n = 3$ (see Eq. **42**), together with those obtained from the direct numerical solution of Eq. **41** are plotted in Fig. 3*C*. Thus, local accumulation times for morphogen gradients in models with superlinear power-law degradation are proportional to the diffusion time and are independent of the kinetic parameters (k_n and n), at least for $n < 5$.

Dependence on the Strength of the Source. Another important difference in the accumulation times in linear and nonlinear problems lies in the dependence on the strength of the source of morphogen production. For the first-order degradation rate law, $\tau_1(x)$ does not depend on the strength of the morphogen production at the boundary; see Eq. **5** (34). This is an immediate consequence of the definition of the relaxation function and the linearity of the problem for $k = k_1$. On the other hand, in the case of second-order degradation, $\tau_2(x)$ depends on the strength of the source. In particular, it is a decreasing function of Q that asymptotically approaches a value that is proportional to the diffusion time; see Eq. **6**. In other words, the accumulation time is insensitive to the strength of the source at large values of Q. The accumulation times computed for problems with higher order of degradation ($n = 3,4$) exhibit the same asymptotic behavior (see *SI Appendix*).

This result has important implications for the robustness of morphogen gradients. Specifically, the steady solutions for problems with $n > 1$ have a similar asymptotic behavior: For large values of Q, the solution at a given x approaches a value that depends on the distance from the source of production, diffusivity, and the degradation rate constant (41) [see also recent work (43) for the case of a stochastic source]. Taken together, the asymptotic behavior of the steady-state concentration and local accumulation time mean that for any x not equal to zero, there is a regime (large values of Q) where the *same* steady-state value is reached in the *same* time.

Discussion

We have developed a systematic analytical approach for characterizing the dynamics of morphogen gradients. Importantly, this approach provides explicit parametric dependence of the time needed to establish a steady-state gradient in reaction–diffusion models of the source–sink mechanism. Our bounds for local accumulation times are in very good *quantitative* agreement (within approximately 30%) with the results of the direct numerical solution of the governing equations. These bounds can, therefore, be considered as counterparts of the exact results obtained in the case of linear problems. Given that the parameters in the underlying models are usually not known to very high accuracy, our analytical bounds represent a practical analog of the exact solution of the problem.

We demonstrated the effectiveness of our approach by deriving two-sided inequalities for the accumulation time in models with superlinear power-law degradation kinetics. The same approach can be readily applied to other types of kinetics. For example, in a number of experimental systems, morphogen degradation is mediated by cell surface receptors that become saturated at high morphogen concentration. The simplest model of this mechanism is given by the following dimensionless reaction–diffusion problem (see *SI Appendix* for details):

$$u_t = u_{xx} - \frac{u}{1+u}, \qquad u_x(0,t) = -\alpha, \qquad u(x,0) = 0, \qquad \textbf{[43]}$$

where α is again proportional to the source strength. Thus, the degradation rate law follows the first- and zeroth-order kinetics at low and high morphogen concentrations, respectively. In this case, the inequalities for the accumulation time can be derived (see *SI Appendix*) and are given explicitly by

$$\frac{x}{2} + \frac{v(0)}{2\alpha} \leq \hat{\tau}_0(x) \leq \frac{x}{2} + \frac{M - Pv(x) - Qxv(x)}{1 + v(x)}, \qquad \textbf{[44]}$$

where M,P,Q are some positive constants depending only on α, and $v(x)$ is the steady state. Similar to the problems with power-law degradation kinetics, these bounds are also in good agreement with the results of the direct numerical solution (Fig. 3*D*). As expected, from this expression one can see that $\hat{\tau}_0(x) \sim x$, for large x, and the asymptotic behavior is precisely the same as for the linear degradation, where $\hat{\tau}_1(x) = \frac{1}{2}(x+1)$.

At this point, our approach can handle only single-variable models of the source–sink mechanism. These scalar models can be viewed as simplified versions of more complex multicomponent models that lead to systems of nonlinear reaction–diffusion equations. For systems of reaction–diffusion partial differential equations, the analysis of the dynamics is complicated by

the general lack of comparison principle, which was essential to our approach. In some nonlinear problems, such as the one that can be classified as monotone systems (see, e.g., ref. 44), our approach may be still be applicable. Morphogen dynamics in other systems, such as the ones where the local kinetics is characterized by overshoots (45–47), may require different analytical tools.

ACKNOWLEDGMENTS. The authors thank J. Briscoe for providing the image for Fig. 1. The work of P.V.G. was supported, in part, by the United States–Israel Binational Science Foundation Grant 2006-151. A.M.B. was supported by the Intramural Research Program of the National Institutes of Health, Center for Information Technology. C.B.M. acknowledges partial support by National Science Foundation (NSF) via Grants DMS-0718027 and DMS-0908279. S.Y.S. acknowledges partial support by NSF via Grant DMS-0718604, by National Institutes of Health via Grant GM078079, and by the NSF Career award.

1. Martinez-Arias A, Stewart A (2002) *Molecular Principles of Animal Development* (Oxford Univ Press, New York).
2. Wolpert L (1969) Positional information and spatial pattern of cellular differentiation. *J Theor Biol* 25:1–47.
3. Wolpert L (1996) One hundred years of positional information. *Trends Genet* 12:359–364.
4. Driever W, Nusslein-Volhard C (1988) A gradient of bicoid protein in drosophila embryos. *Cell* 54:83–93.
5. Steward R (1989) Relocalization of the dorsal protein from the cytoplasm to the nucleus correlates with its function. *Cell* 59:1179–1188.
6. Rushlow CA, Han KY, Manley JL, Levine M (1989) The graded distribution of the dorsal morphogen is initiated by selective nuclear transport in drosophila. *Cell* 59:1165–1177.
7. Roth S, Stein D, Nusselin-Volhard C (1989) A gradient of nuclear-localization of the dorsal protein determines dorsoventral pattern in the drosophila embryo. *Cell* 59:1189–1202.
8. Tabata T, Takei Y (2004) Morphogens, their identification and regulation. *Development* 131:703–712.
9. Dyson S, Gurdon JB (1998) The interpretation of position in a morphogen gradient as revealed by occupancy of activin receptors. *Cell* 93:557–568.
10. Ashe HL, Briscoe J (2006) The interpretation of morphogen gradients. *Development* 133:385–394.
11. Lander AD (2007) Morpheus unbound: Reimagining the morphogen gradient. *Cell* 128:245–256.
12. Wartlick O, Kicheva A, Gonzalez-Gaitan M (2009) Morphogen gradient formation. *Cold Spring Harbor Perspect Biol*, 1 p:a001255.
13. Lander AD, Nie Q, Wan FY (2002) Do morphogen gradients arise by diffusion? *Dev Cell* 2:785–796.
14. Kicheva A, et al. (2007) Kinetics of morphogen gradient formation. *Science* 315:521–525.
15. Yu SR, et al. (2009) Fgf8 morphogen gradient forms by a source-sink mechanism with freely diffusing molecules. *Nature* 461:533–536.
16. Briscoe J (2009) Making a grade: Sonic hedgehog signalling and the control of neural cell fate. *EMBO J* 28:457–465.
17. Chen Y, Struhl G (1996) Dual roles for patched in sequestering and transducing hedgehog. *Cell* 87:553–563.
18. Incardona JP, et al. (2000) Receptor-mediated endocytosis of soluble and membrane-tethered sonic hedgehog by patched-1. *Proc Natl Acad Sci USA* 97:12044–12049.
19. Dessaud E, McMahon AP, Briscoe J (2008) Pattern formation in the vertebrate neural tube: A sonic hedgehog morphogen-regulated transcriptional network. *Development* 135:2489–2503.
20. Lander AD, Nie Q, Vargas B, Wan FYM (2005) Aggregation of a distributed source in morphogen gradient formation. *Stud Appl Math* 114:343–374.
21. Lander AD, Nie Q, Wan FY (2006) Internalization and end flux in morphogen gradient formation. *J Comput Appl Math* 190:232–251.
22. Bergmann S, et al. (2007) Pre-steady-state decoding of the bicoid morphogen gradient. *PLoS Biol* 5:e232–242.
23. Saunders T, Howard M (2009) When it pays to rush: Interpreting morphogen gradients prior to steady-state. *Phys Biol* 6:046020.
24. Gregor T, Wieschaus EF, McGregor AP, Bialek W, Tank DW (2007) Stability and nuclear dynamics of the bicoid morphogen gradient. *Cell* 130:141–152.
25. Kanodia JS, et al. (2009) Dynamics of the dorsal morphogen gradient. *Proc Natl Acad Sci USA* 106:21707–21712.
26. Simeoni I, Gurdon JB (2007) Interpretation of BMP signaling in early Xenopus development. *Dev Biol* 308:82–92.
27. Kinoshita T, Jullien J, Gurdon JB (2006) Two-dimensional morphogen gradient in Xenopus: Boundary formation and real-time transduction response. *Dev Dynam* 235:3189–3198.
28. Bourillot PY, Garrett N, Gurdon JB (2002) A changing morphogen gradient is interpreted by continuous transduction flow. *Development* 129:2167–2180.
29. McDowell N, Gurdon JB, Grainger DJ (2001) Formation of a functional morphogen gradient by a passive process in tissue from the early Xenopus embryo. *Int J Dev Biol* 45:199–207.
30. Hagemann AI, Xu X, Nentwich O, Hyvonen M, Smith JC (2009) Rab5-mediated endocytosis of activin is not required for gene activation or long-range signalling in Xenopus. *Development* 136:2803–2813.
31. Williams PH, Hagemann AI, González-Gaitán M, Smith JC (2004) Visualizing long-range movement of the morphogen Xnr2 in the Xenopus embryo. *Curr Biol* 14:1916–1923.
32. Kutejova E, Kicheva A, Briscoe J (2009) Temporal dynamics of patterning by morphogen gradients. *Curr Opin Genet Dev* 19:315–322.
33. Crick F (1970) Diffusion in embryogenesis. *Nature* 225:420–422.
34. Berezhkovskii AM, Sample C, Shvartsman SY (2010) How long does it take to establish a morphogen gradient. *Biophys J* 99:L59–L61.
35. Fife PC (1979) *Mathematical Aspects of Reacting and Diffusing Systems* (Springer, Berlin).
36. Aronson DG, Weinberger HF (1975) *Proceedings of the Tulane Program in Partial Differential Equations and Related Topics, Lecture Notes in Mathematics*, ed JA Goldstein Vol 446 (Springer, Berlin), pp 5–49.
37. Smoller J (1983) *Shock Waves and Reaction-Diffusion Equations* (Springer, New York).
38. Protter MH, Weinberger HF (1984) *Maximum Principles in Differential Equations* (Springer, New York).
39. Sattinger DH (1972) Monotone methods in nonlinear elliptic and parabolic boundary value problems. *Indiana U Math J* 21:979–1000.
40. Walter W (2002) Nonlinear parabolic differential equations and inequalities. *Disc Cont Dyn Syst* 8:451–468.
41. Eldar A, Rosin D, Shilo BZ, Barkai N (2003) Self-enhanced ligand degradation underlies robustness of morphogen gradients. *Dev Cell* 5:635–646.
42. Rudin W (1970) *Real and Complex Analysis* (McGraw–Hill, London).
43. Varadhan SRS, Zygouras N (2008) Behavior of the solution of a random semilinear heat equation. *Commun Pur Appl Math* 61:1298–1329.
44. Volpert AI, Volpert VA, Volpert VA (1994) *Traveling Wave Solutions of Parabolic Systems* (American Mathematical Society, Providence, RI).
45. Eldar A, et al. (2002) Robustness of the BMP morphogen gradient in *Drosophila* embryonic patterning. *Nature* 419:304–308.
46. Mizutani CM, et al. (2005) Formation of the BMP activity gradient in the *Drosophila* embryo. *Dev Cell* 8:915–924.
47. Shimmi O, Umulis D, Othmer H, O'Connor MB (2005) Facilitated transport of a Dpp/Scw heterodimer by Sog/Tsg leads to robust patterning of the *Drosophila* blastoderm embryo. *Cell* 120:873–886.